



Effects of Hole Locations on the Elastic Global Buckling Loads of Cold-Formed Steel Channel Members with Perforations Under Compression or Bending

Ngoc Hieu Pham^(✉)

Faculty of Civil Engineering, Hanoi Architectural University, Hanoi, Vietnam
hieupn@hau.edu.vn

Abstract. Cold-formed steel members with perforations have been commonly applied to meet the demands for technical installations. The design of the perforated members was regulated in Specification AISI S100-16 using the Direct Strength Method (DSM). This method is based on elastic buckling analyses to predict the capacities of cold-formed steel members. The determination of elastic buckling loads is compulsory for the application of the DSM method in the design and has been presented in the Specification. The specification regulations are only applied for symmetrical and evenly spaced holes. The paper, therefore, investigates the effects of unsymmetrical, unevenly spaced and eccentric holes on the elastic global buckling loads of perforated channel members using finite element analyses. The effect of symmetrical and evenly web holes on the elastic global buckling loads of cold-formed steel channel members in comparison with those of gross section members is also investigated.

Keywords: Hole locations · Elastic global buckling loads · Cold-formed steel channel members · Perforations

1 Introduction

Web holes are found in a variety of cold-formed steel members to allow technical services to pass through. These holes are commonly pre-punched in the webs of channel or Zed sections that have significant impacts on the stability and capacity of this type of structural member. The design of the cold-formed steel members with holes was also included in the Specification AISI S100-16 [1] using the Direct Strength Method (DSM). The DSM method can provide the sectional and member capacities based on the elastic buckling loads. The determination of the elastic buckling loads, therefore, is mandatory for the design of perforated members.

A large number of studies on the cold-formed steel members with perforations have been available in literature. An experimental program presented in [2] investigated the strength of stub columns with circular holes to illustrate the strength decreasing with the increasing of hole diameter. The influences of circular, slotted and rectangular web holes

on the strengths of stub columns were also investigated by many studies [3–5]. A variety of studies carried out by Moen and Schafer [6–13] to study the stability and capacity of cold-formed steel members with holes. These studies were the base to propose a simple method to determine the elastic sectional and global buckling loads of perforated members and the DSM design formulae for the design of perforated members. These proposals were then included in the Specification AISI S100-16 [1]. In order to support the elastic buckling analyses of perforated sections, a simple hole module was developed by the American Iron and Steel Institute [14] to perform the elastic buckling analysis and obtain the elastic buckling loads of perforated sections that can be used for the DSM design. Moen and Yu [15, 16] studied the elastic buckling analysis of cold-formed members with edge-stiffened holes. These previous studies were aimed to investigate the stability and the capacities of perforated members with symmetrical and evenly spaced holes whereas studies on asymmetric and unevenly web holes remain scarce.

The influences of hole locations on the capacities of stub columns were reported in [17–19] and the effects of hole lengths on the behaviors of compression elements were studied in [20]. Ortiz-Colberg [2] carried out 25 intermediate column tests and pointed out that the column strengths were not impacted by a single hole along the length of the column tests. Moen and Schafer [6] investigate the effects of the locations of a single hole on the elastic buckling of an intermediate column length. Their research demonstrated that the locations of the single hole have a minimal impact on the elastic buckling loads of the investigated columns. The influence of unsymmetrical and unevenly web holes of the elastic buckling loads of long perforated members are not reported. This paper, therefore, investigates the effects of unevenly spaced and/or unsymmetrical web holes or eccentric web holes on the elastic global buckling loads of long perforated members under compression or bending using finite element analyses. The finite element models used for this investigation were verified against test results as presented in Pham *et al.* [21, 22]. Also, the influence of symmetrical and evenly web holes on the elastic global buckling loads of cold-formed steel channel members in comparison with those of gross section members according to the specification AISI S100-16 [1] is included.

2 Finite Element Models for Buckling Analyses

Material properties are used for the investigation including Young's modulus $E = 203400$ MPa and Poisson's constant $\mu = 0.3$. The finite element models for buckling analyses were developed and validated against the test results as fully reported in Pham *et al.* [21, 22] including compression and bending models.

In terms of compression models, two model configurations were constructed with the variations of end boundary conditions to obtain different global buckling modes. The first configuration allows the specimens to freely rotating about the minor axis to achieve the flexural buckling mode whereas the free rotation about the major axis was used for the second configuration to obtain the flexural-torsional buckling mode. Warping displacements were prevented at two ends for both two configurations. These configuration models are illustrated in Fig. 1 and Fig. 2. The effective lengths, therefore, were taken as $L_x = L_z = 0.5 L$; $L_y = L$ and $L_y = L_z = 0.5L$; $L_x = L$ for the first and second configurations respectively, where L is the member length. The lateral load was applied at the centroid of one end section.

In terms of the bending model, the web of each end section was contacted with three points through the shear centre of the section. The model configuration was developed with simple supports and free warping displacements, as illustrated in Fig. 3. The effective lengths were taken as $L_x = L_y = L_z = L$, where L is the member length. Vertical loads were applied at the shear centres (see loading points in Fig. 3) of the section.

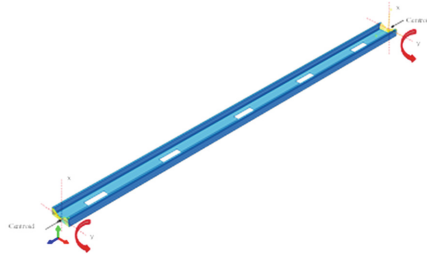


Fig. 1. The flexural buckling model under compression

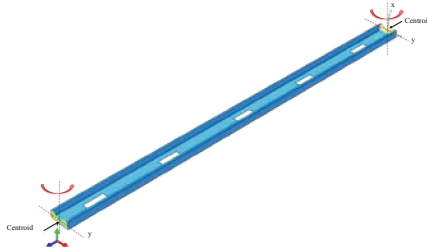


Fig. 2. The flexural-torsional buckling model under compression

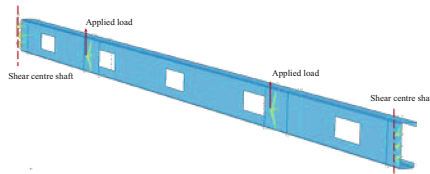


Fig. 3. The flexural-torsional buckling model under bending

3 Effects of Symmetrical and Evenly Spaced Web Holes on the Elastic Global Buckling Loads of Cold-Formed Steel Channel Members

The global buckling loads of perforated members can be determined using the “weighted average” method as regulated in AISI S100-16 [1]. The elastic global buckling loads of a column include the flexural or flexural-torsional buckling loads as presented in Eqs. (1) and (2), whereas the global buckling moment of a flexural member is determined as in Eq. (3).

The elastic flexural buckling load of a compressive member:

$$P_{cre} = \frac{\pi^2 EI_{y,avg}}{(K_y L)^2} \quad (1)$$

The elastic flexural-torsional buckling load of a compressive member:

$$P_{cre} = \frac{1}{2\beta} \left[(P_{ex} + P_t) - \sqrt{(P_{ex} + P_t)^2 - 4\beta P_{ex} P_t} \right] \quad (2)$$

The elastic flexural-torsional buckling moment of a flexural member:

$$M_{cre} = \frac{\pi}{K_y L} \sqrt{EI_{y,avg} \left(GJ_{avg} + \frac{\pi^2 EC_{w,net}}{(K_t L)^2} \right)} \quad (3)$$

where

$$P_{ex} = \frac{\pi^2 EI_{x,avg}}{(K_x L)^2}; \quad P_t = \frac{1}{r_{o,avg}^2} \left(GJ_{avg} + \frac{\pi^2 EC_{w,net}}{(K_t L)^2} \right)$$

$I_{x,avg}$, $I_{y,avg}$, J_{avg} , $r_{o,avg}$ are the section properties determined using the “weighted average” method as regulated in AISI S100-16, as follows:

$$I_{avg} = \frac{I_g L_g + I_{net} L_{net}}{L}; \quad J_{avg} = \frac{J_g L_g + J_{net} L_{net}}{L}; \quad r_{o,avg} = \sqrt{x_{o,avg}^2 + y_{o,avg}^2 + \frac{I_{x,avg} + I_{y,avg}}{A_{avg}}}$$

$$A_{avg} = \frac{A_g L_g + A_{net} L_{net}}{L}; \quad x_{o,avg} = \frac{x_{o,g} L_g + x_{o,net} L_{net}}{L}; \quad y_{o,avg} = \frac{y_{o,g} L_g + y_{o,net} L_{net}}{L}$$

$(I_g, J_g, A_g, L_g, x_{o,g}, y_{o,g})$ and $(I_{net}, J_{net}, A_{net}, L_{net}, x_{o,net}, y_{o,net})$ are properties of the gross section and the net section respectively.

$C_{w,net}$ is the net warping constant of an assumed section with the assumed depth of the hole (h_{hole*}) determined in Eq. (4), where h_{hole} is the actual depth of the hole and D is the depth of the section.

$$h_{hole*} = h_{hole} + \frac{1}{2}(D - h_{hole}) \left(\frac{h_{hole}}{D} \right)^{0,2} \quad (4)$$

The C20015 section is selected for this investigation with the nominal dimensions including $D = 203$ mm, $B = 76$ mm, $L = 19.5$ mm, $t = 1.5$ mm, as demonstrated in

Fig. 4. The investigated member has a length of 2.5 m and 05 symmetrical and evenly spaced web holes with the hole depth h_{hole} varying from 0.2 to 0.8 times of the section depth and the hole length varying from 0.5 to 2 times of the section depth. The spacing between these web holes are illustrated in Fig. 5. The loads and boundary conditions have been presented in Sect. 2. The elastic global buckling loads of the perforated members are determined using the “weight average” method and plotted into the graphs in Figs. 6, 7 and 8 in comparison with those of gross section members.

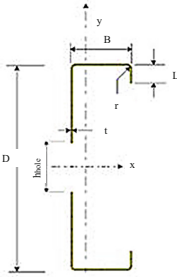


Fig. 4. Nomenclature and nominal dimensions for C20015 section

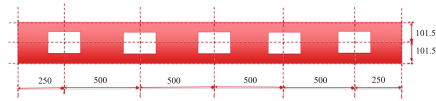


Fig. 5. The locations of symmetrical and evenly spaced web holes

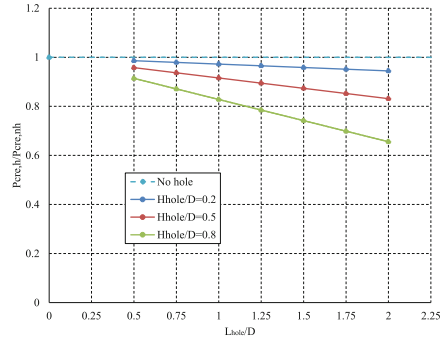
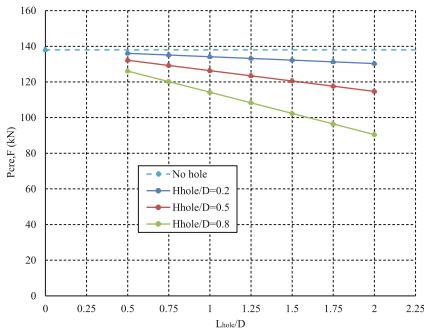


Fig. 6. Flexural buckling loads under compression ($P_{cre,F}$ is the flexural buckling load; $P_{cre,h}$ and $P_{cre,th}$ are elastic global buckling loads of the gross section and the net section.)

The investigated results show that the elastic global buckling loads decrease as the hole sizes increase, relative to the web depth. The relationship between buckling loads and the hole lengths is linear, interpolation then can be used to determine the buckling loads of the intermediate points between the specific points of the hole lengths.

The web holes were found to have the most significant impacts on the flexural-torsional buckling loads under compression with the reduction of nearly 50% compared to those of the gross section, whereas these reduction values are about 30% for both the flexural mode due to compression and the flexural-torsional buckling mode under bending.

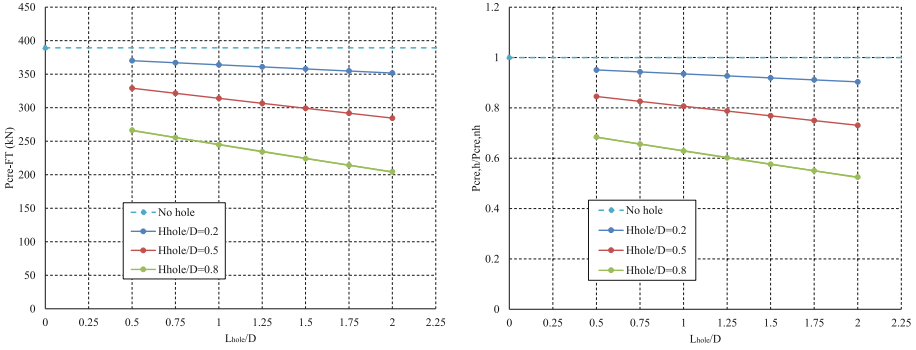


Fig. 7. Flexural-torsional buckling loads under compression ($P_{cre,FT}$ is the flexural-torsional buckling load; $P_{cre,h}$ and $P_{cre,nh}$ are elastic global buckling loads of the gross section and the net section.)

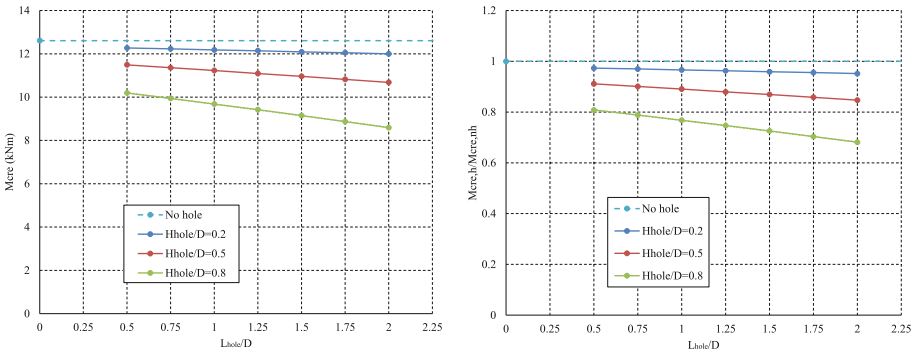


Fig. 8. Flexural-torsional buckling moments under bending ($M_{cre,FT}$ is the flexural-torsional buckling moment; $M_{cre,h}$ and $M_{cre,nh}$ are elastic global buckling loads of the gross section and the net section.)

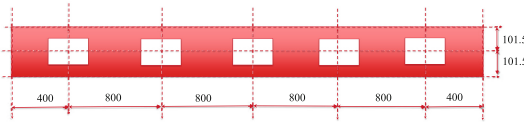


Fig. 9. The original model - Model 0

The variation of hole lengths has insignificant impacts on the elastic global buckling loads if the hole depths are small (see $h_{hole}/D = 0.2$ in the graphs) with the small slopes of the relationship lines. In terms of the large hole depths (see $h_{hole}/D = 0.8$ in the graphs), these slopes significantly increase to demonstrate the noticeable influences of the hole lengths on the elastic global buckling loads.

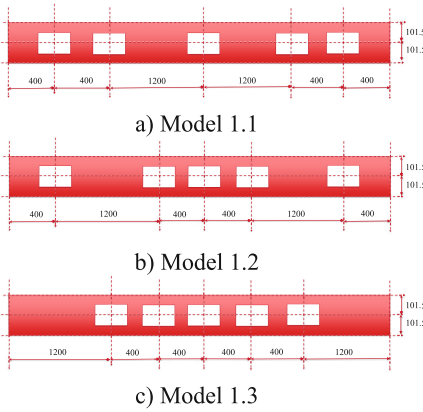


Fig. 10. Model 1 – Symmetrical holes

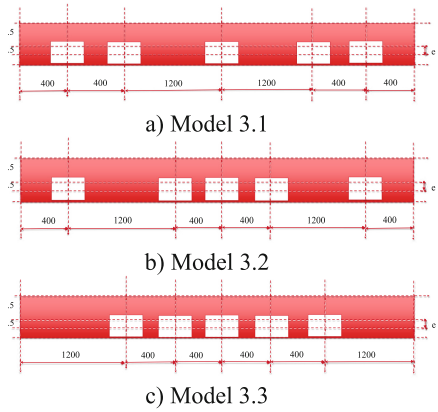


Fig. 11. Model 3 – Symmetrical and eccentric holes

4 Effects of Web Hole Locations on the Elastic Global Buckling Loads of Perforated Channel Members

The investigated section is the C20030 section with the nominal dimensions including $D = 203$; $B = 76$; $L = 19.5$; $t = 3$, and the nomenclature of this section is illustrated in Fig. 4. The member length is taken as 4000 for investigation. The thickness and the length of the investigated member are selected to obtain the global buckling modes without the interactions with other sectional modes. The finite element models used in this investigation are presented in Sect. 2.

There are 05 rectangular holes in the web of the section with the ratio of hole length and section depth (L_{hole}/D) of 1.0 and the ratios of hole depth and section depth (h_{hole}/D) varying from 0.2 to 0.8. The spacings and locations of these holes are initially symmetrical and even (see Fig. 9), are then rearranged as illustrated in Figs. 10, 11, 12 and 13 to investigate the effects of unsymmetrical, unevenly spaced and eccentric holes on the elastic global buckling loads of channel members under compression or bending. The eccentric values (e) are $0.25D$, $0.125D$ and $0.05D$ for the ratios of h_{hole}/D varying from 0.2, 0.5 to 0.8 respectively. Failure modes are obtained as illustrated in Figs. 14, 15 and 16, and the deviation of buckling loads (in percentage) between investigated models (Model 1 to Model 4) and the original model (Model 0) are illustrated in Fig. 17.

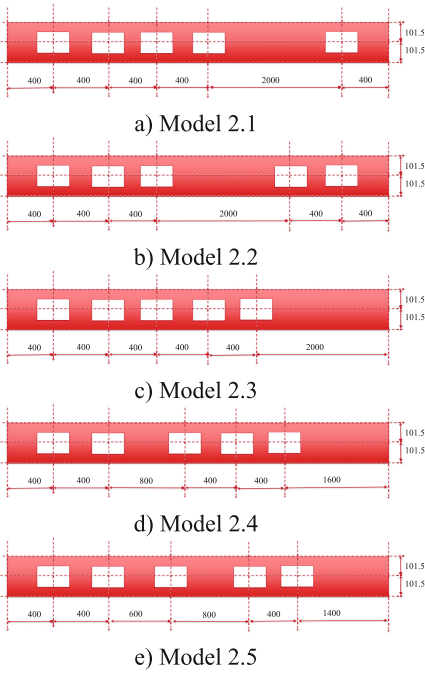


Fig. 12. Model 2 – Unsymmetrical holes

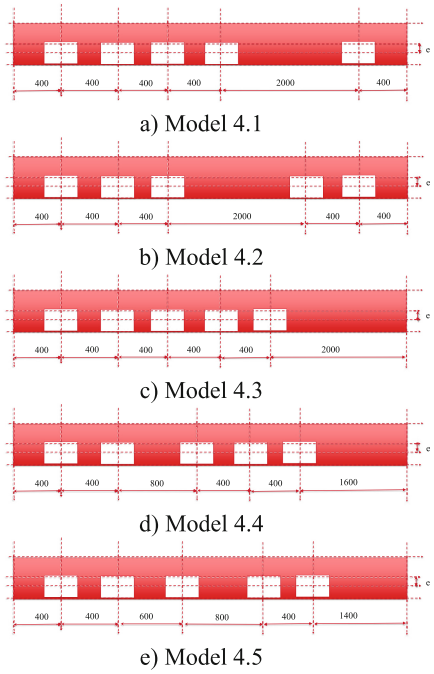


Fig. 13. Model 4 – Unsymmetrical and eccentric holes

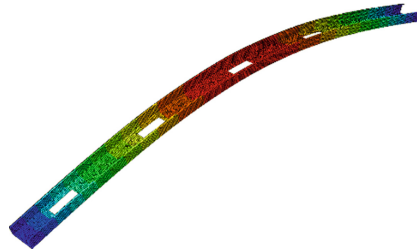


Fig. 14. Flexural buckling mode under compression

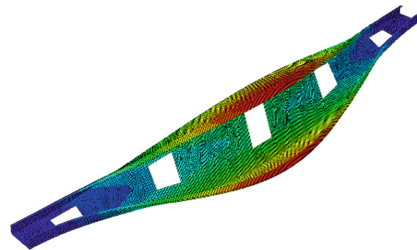


Fig. 15. Flexural-torsional buckling mode under compression

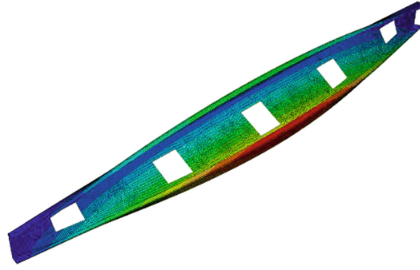


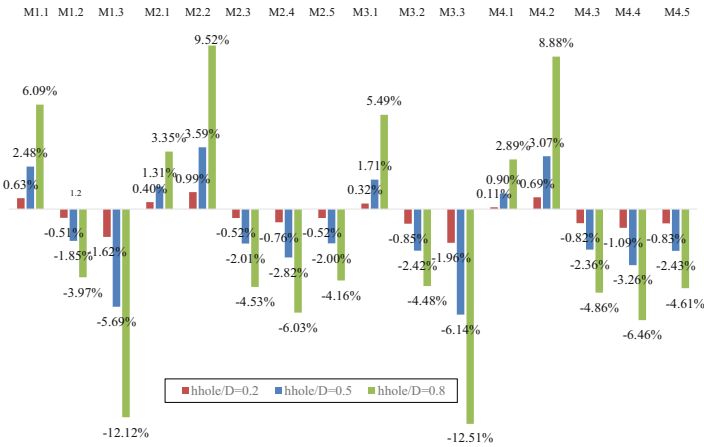
Fig. 16. Flexural-torsional buckling mode under bending

The investigated results illustrate that the web hole locations have a minimal influence on the elastic global buckling of perforated members for the small hole depth ($h_{hole}/D = 0.2$), but it becomes significant impacts for the large hole ($h_{hole}/D = 0.8$).

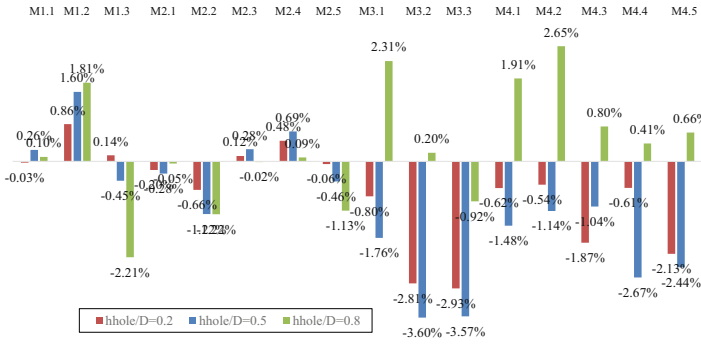
In terms of compression, the deviation is less than 3% for the flexural-torsional buckling mode regarding the hole depths whereas it reaches 12% for the flexural buckling mode with the large hole ($h_{hole}/D = 0.8$). The simple method for the determination of elastic global buckling loads for symmetrical and evenly spaced holes, therefore, can be applied to this flexural-torsional buckling mode.

The results show that the elastic global buckling loads significantly decrease as the web holes are arranged closely to the mid-length. This conclusion can be seen in the results of Models 1.3 and 3.3 for both compression and bending.

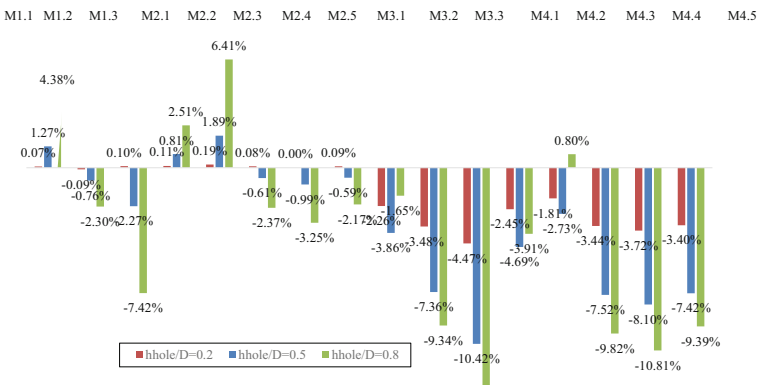
The buckling loads are noticeable increase with the absence of the web hole at the mid-length as seen in the results of Models 2.2 and 4.2. This illustrates the great impact of the web hole at the mid-length on the elastic global buckling of perforated members.



a) The flexural buckling mode under compression



b) The flexural-torsional buckling mode under compression



c) The flexural-torsional buckling mode under bending

Fig. 17. The deviation of buckling loads between the Model 1 to Model 4 and the Model 0

5 Conclusion

The paper investigated the effects of web holes on the elastic global buckling loads of cold-formed steel channel members under compression or bending. The effects of symmetrical and evenly spaced web holes on the elastic global buckling of cold-formed steel channel members were carried out using the simple method according to the Specification AISI S100-16 with the following conclusions: as the sizes of holes increased, the elastic buckling loads of perforated members decreased. In terms of the high ratio of the hole depth and the section depth, the elastic buckling loads were observed to be significantly reduced as the hole length increased.

The influences of hole locations on the elastic global buckling loads were investigated by using finite element analyses. The finite element models were validated in previous studies of Pham *et al.* [21, 22], and they were used for elastic buckling analyses in this investigation. Based on the investigated results, the following conclusions can be drawn:

- The “weighted average” method in the AISI S100 still can be used to determine the elastic flexural-torsional buckling loads under compression due to the minimal impacts of hole locations.
- The presence of the web hole at the mid-length has great impacts on the elastic global buckling loads of perforated channel members under compression or bending.

These remarks are beneficial for the designers in selecting the sizes and locations of the web holes in the design.

References

1. American Iron and Steel Institute: North American Specification for the Design of Cold-formed Steel Structural Members. American Iron and Steel Institute, Washington DC (2016)
2. Ortiz-Colberg, R.A.: The Load Carrying Capacity of Perforated Cold-Formed Steel Columns. Cornell University, Ithaca (1981)
3. Sivakumanran, K.S.: Load capacity of uniformly compressed cold-formed steel section with punched web. *Can. J. Civil Eng.* **14**(4), 8 (1987). <https://doi.org/10.1139/187-080>
4. Banwait, A.S.: Axial Load Behaviour of Thin-Walled Steel Sections with Openings. McMaster, University Hamilton, Ontario (1987)
5. Abdel-Rahman, N.: Cold-Formed Steel Compression Members with Perforations. McMaster, University Hamilton, Ontario (1997)
6. Moen, C.D.: Direct Strength Design for Cold-Formed Steel Members with Perforations. Johns Hopkins University, Baltimore (2008)
7. Moen, C.D., Schafer, B.W.: Experiments on cold-formed steel columns with holes. *Thin-Wall Struct.* **46**(10), 1164–1182 (2008). <https://doi.org/10.1016/j.tws.2008.01.021>
8. Moen, C.D., Schafer, B.W.: Elastic buckling of cold-formed steel columns and beams with holes. *Eng. Struct.* **31**, 2812–2824 (2009). <https://doi.org/10.1016/j.engstruct.2009.07.007>
9. Moen, C.D., Schafer, B.W.: Impact of holes on the elastic buckling of cold-formed steel columns. In: International Specialty Conference on Cold-Formed Steel Structures, pp. 269–283 (2006)

10. Moen, C.D., Schafer, B.W.: Extending direct strength design to cold-formed steel beams with holes. In: The 20th International Specialty Conference on Cold-Formed Steel Structures - Recent Research and Developments in Cold-Formed Steel Design and Construction, pp. 171–183 (2010)
11. Cai, J., Moen, C.D.: Elastic buckling analysis of thin-walled structural members with rectangular holes using generalized beam theory. *Thin-Walled Struct.* **107**, 274–286 (2016). <https://doi.org/10.1016/j.tws.2016.06.014>
12. Moen, C.D., Schafer, B.W.: *Direct Strength Design of Cold-Formed Steel Members with Perforations*. Johns Hopkins University, Baltimore (2009)
13. Moen, C.D., Schafer, B.W.: Elastic buckling of thin plates with holes in compression or bending. *Thin-Walled Struct.* **47**(12), 1597–1607 (2009). <https://doi.org/10.1016/j.tws.2009.05.001>
14. American Iron and Steel Institute: *Development of CUFSM Hole Module and Design Tables for the Cold-formed Steel Cross-sections with Typical Web Holes in AISI D100*. Research Report, American Iron and Steel Institute (2021)
15. Moen, C.D., Yu, C.: Elastic buckling of thin-walled structural components with edge-stiffened holes. In: *Collection of Technical Papers - AIAA/ASME/ASCE/AHS/ASC Structures, Structural Dynamics and Materials Conference*, pp. 1–10 (2010)
16. Grey, C.N., Moen, C.D.: Elastic buckling simplified methods for cold-formed columns and beams with edge-stiffened holes. In: *Structural Stability Research Council Annual Stability Conference*, pp. 92–103 (2011)
17. Rhodes, J., Schneider, F.D.: The compressional behaviour of perforated elements. In: *Twelfth International Specialty Conference on Cold-Formed Steel Structures*, pp. 11–28 (1994)
18. Loov, R.: Local buckling capacity of C-shaped cold-formed steel sections with punched webs. *Can. J. Civil Eng.* **11**(1), 1–7 (1984). <https://doi.org/10.1139/l84-001>
19. Pu, Y., Godley, M.H.R., Beale, R.G., Lau, H.H.: Prediction of ultimate capacity of perforated lipped channels. *J. Struct. Eng.* **125**(5), 4 (1999). [https://doi.org/10.1061/\(ASCE\)0733-9445\(1999\)125:5\(510\)](https://doi.org/10.1061/(ASCE)0733-9445(1999)125:5(510))
20. Rhodes, J., Macdonald, M.: The effects of perforation length on the behaviour of perforated elements in compression. In: *Thirteenth International Specialty Conference on Cold-Formed Steel Structures*, pp. 91–101 (1996)
21. Pham, N.H., Pham, C.H., Rasmussen, K.J.R.: Finite element simulation of member buckling of cold-rolled aluminium alloy 5052 channel columns. In: Ha-Minh, C., et al. (eds.) *CIGOS 2019, Innovation for Sustainable Infrastructure: Proceedings of the 5th International Conference on Geotechnics, Civil Engineering Works and Structures*, pp. 263–268. Springer Singapore, Singapore (2020). https://doi.org/10.1007/978-981-15-0802-8_39
22. Pham, N.H., Pham, C.H., Rasmussen, K.J.R.: Numerical investigation of the member buckling of cold-rolled aluminium alloy channel beams. In: *The 9th International Conference on Steel and Aluminium Structures*, p. 11 (2019)

Open Access This chapter is licensed under the terms of the Creative Commons Attribution 4.0 International License (<http://creativecommons.org/licenses/by/4.0/>), which permits use, sharing, adaptation, distribution and reproduction in any medium or format, as long as you give appropriate credit to the original author(s) and the source, provide a link to the Creative Commons license and indicate if changes were made.

The images or other third party material in this chapter are included in the chapter's Creative Commons license, unless indicated otherwise in a credit line to the material. If material is not included in the chapter's Creative Commons license and your intended use is not permitted by statutory regulation or exceeds the permitted use, you will need to obtain permission directly from the copyright holder.

